Available online at www.sciencedirect.com
ScienceDirect
Journal of Solid State Chemistry 180 (2007) 2510–2516
JOURNAL OF SOLID STATE CHEMISTRY
www.elsevier.com/locate/jssc

Controlled synthesis of bismuth oxo nanoscale crystals (BiOCl, $Bi_{12}O_{17}Cl_2$, α-Bi_2O_3, and $(BiO)_2CO_3$) by solution-phase methods

Xiang Ying Chen, Hyun Sue Huh, Soon W. Lee*

Department of Chemistry (BK21), Sungkyunkwan University, Natural Science Campus, Suwon 440-746, South Korea

Received 22 April 2007; received in revised form 2 June 2007; accepted 3 June 2007
Available online 10 July 2007

Abstract

We present the controlled solution-phase synthesis of several sheet- or rod-like bismuth oxides, BiOCl, $Bi_{12}O_{17}Cl_2$, α-Bi_2O_3 and $(BiO)_2CO_3$, by adjusting growth parameters such as reaction temperature, mole ratios of reactants, and the base used. BiOCl, $Bi_{12}O_{17}Cl_2$, and α-Bi_2O_3 could be prepared from $BiCl_3$ and NaOH, whereas $(BiO)_2CO_3$ was prepared from $BiCl_3$ and urea. BiOCl and $Bi_{12}O_{17}Cl_2$ could also be prepared from $BiCl_3$ and ammonia. The α-Bi_2O_3 sample exhibited strong emission at room temperature.

Keywords: Bismuth compounds; Solution-phase; Nanostructures; Photoluminescence

1. Introduction

Recent research efforts have been focused on the fabrication of nanometer- and micrometer-size anisotropic materials due to their unique and desirable properties applicable to various fields, which are basically affected by their shapes, sizes, and phases. Besides the conventional one-dimensional (1-D) nanostructures (nanorods, nanowires, and nanotubes), many 2-D nanostructures such as nanosheets and nanoplates have been prepared recently [1,2]. These nanostructures possess good crystallinity, high anisotropy with an ultrathin thickness as well as the enhanced properties [3]. However, particularly in the case of bismuth-based multi-component compounds with sheet- or plate-like morphologies, the controlled synthetic study is still unexplored.

Bismuth oxychlorides such as BiOCl, $Bi_4O_5Cl_2$, $Bi_{24}O_{31}Cl_{10}$, Bi_3O_4Cl, and $Bi_{12}O_{17}Cl_2$ have been widely studied [4]. For example, BiOCl exhibits catalytic properties for the oxidative cracking of *n*-butane to lower alkenes [5]. However, current synthetic barriers to these compounds hinder us from systematically investigating them. Bismuth trioxide (Bi_2O_3) with α, β, γ, or δ phase has excellent electrical [6], optical [7], photocatalytic [8], or conducting [9] properties. Interestingly, $(BiO)_2CO_3$ has antibacterial properties against *Helicobacter pylori* [10,11].

BiOCl nanosheets or single crystals were recently synthesized by the solution-based methods [12,13]. In particular, Kaskel and co-workers prepared BiO*X* (*X* = Cl, Br, I) nanoparticles by the reverse microemulsion methods [14]. In addition, bismuth oxychloride flakes, fibers, and particles ($Bi_4O_5Cl_2$, $Bi_{24}O_{31}Cl_{10}$, Bi_3O_4Cl, and $Bi_{12}O_{17}Cl_2$) were fabricated under hydrothermal conditions at 350–550 °C [15]. For example, Li and co-workers prepared bismuth oxyhalide nanobelts and nanotubes by finely tuning pH in solution, using CTAB or CTAC as a halide source [16,17]. On the other hand, 1-D α-Bi_2O_3 nanorods [18,19], β-Bi_2O_3 nanowires and nanotubes [20,21], and δ-Bi_2O_3 nanotubes [22] were prepared by the traditional solid-state methods. By contrast, a couple of papers [23,24] reported the nanometer- and micrometer-size α-Bi_2O_3 prepared by the solution-phase methods. However, to our best knowledge, no systematic investigation on the controllable synthesis of BiOCl, $Bi_{12}O_{17}Cl_2$, α-Bi_2O_3, and $(BiO)_2CO_3$ has been carried out via a facile solution-phase route.

In this study, we have systematically investigated growth parameters in preparing bismuth oxides and oxychlorides,

*Corresponding author. Fax: +82 31 290 7075.
E-mail address: swlee@chem.skku.ac.kr (S.W. Lee).

0022-4596/$ - see front matter © 2007 Elsevier Inc. All rights reserved.
doi:10.1016/j.jssc.2007.06.030

BiOCl, $Bi_{12}O_{17}Cl_2$, α-Bi_2O_3, and $(BiO)_2CO_3$, under solution-phase conditions. Our study revealed that reaction temperature, mole ratios of reactants, and the nature of a base (NaOH, urea, or ammonia) were critical to determining the phases of the final products. In particular, the rod-like α-Bi_2O_3 sample exhibited strong emission at room temperature.

2. Experimental

All reactions were carried out in a 100 ml Teflon-lined stainless autoclave at the designated temperature for 12 h. All products were prepared in EtOH–H_2O (1:1, v/v) by controlling the amount of a base (NaOH, urea, or ammonia), reaction temperature, and mole ratios of reactants.

2.1. A typical procedure for the preparation of α-Bi_2O_3

$BiCl_3$ (2 mmol) was dissolved in absolute ethanol (20 ml) with continuous stirring, and then 1.8 M NaOH solution (20 ml) was added to this solution to give yellow precipitates. The solution was further stirred for 20 min and transferred into the autoclave, which was then sealed and kept at 120 °C. After 12 h, the resulting yellow product was filtered off, washed with distilled water (3 × 100 ml) and absolute ethanol (2 × 40 ml), and then dried under vacuum at 60 °C for 6 h.

2.2. Characterization

X-ray powder diffraction (XRPD) patterns were obtained on a Rigaku Max-2200 with filtered Cu *K*α radiation. Transmission electron microscope (TEM) and high resolution transmission electron microscope (HRTEM) images were taken with a JEOL 2100F unit operated at 200 kV at Cooperative Center for Research Facilities (CCRF) in Sungkyunkwan University. Photoluminescence (PL) analysis was recorded with an AB2 spectrophotometer (Amico Bowmann).

3. Results and discussions

By XRPD, we examined the phase, crystallinity, and purity of the samples obtained at 120 °C for 12 h in various mole ratios ($BiCl_3$/NaOH) in EtOH–H_2O (1:1, v/v). Fig. 1a shows the typical XRPD pattern of the sample prepared in the absence of NaOH, whose reflection peaks can be unambiguously indexed as tetragonal BiOCl (*P*4/*nmm*, $a = 3.89$ Å and $c = 7.36$ Å, JCPDS 06-0249). The XRPD pattern in Fig. 1b of the sample prepared in the mole ratio of 1:2 is practically the same as that in Fig. 1a. However, in the mole ratio range of 1:6–1:10, tetragonal $Bi_{12}O_{17}Cl_2$ ($a = 5.44$ Å and $c = 35.20$ Å, JCPDS 37-0702) is a single product (Figs. 1c–e and 2a).

In the mole ratio of 1:12, a mixture of tetragonal $Bi_{12}O_{17}Cl_2$ (major) and monoclinic α-Bi_2O_3 (JCPDS 41-1449) is formed (Fig. 2b). In the very high mole ratios (1:16 and 1:18), pure monoclinic α-Bi_2O_3 (*P*$2_1/c$, $a = 5.84$ Å, $b = 8.16$ Å and $c = 7.51$ Å, JCPDS 41-1449) is obtained (Fig. 2d and e). The XRPD patterns in Figs. 1 and 2 tell us that the initial mole ratio ($BiCl_3$/NaOH) can control the selective formation of BiOCl, $Bi_{12}O_{17}Cl_2$, or α-Bi_2O_3 in EtOH–H_2O.

We also examined the effects of reaction temperature on the selective preparation of the bismuth oxychlorides. Fig. 3 show the XRPD patterns of the samples prepared at various reaction temperatures in a fixed mole ratio ($BiCl_3$/NaOH = 1:18). The sample prepared at 40 °C is a mixture of tetragonal $Bi_{12}O_{17}Cl_2$ and monoclinic α-Bi_2O_3 (Fig. 3a). As the reaction temperature increases from 40 to 100 °C, the amount of α-Bi_2O_3 in the product gradually becomes larger (Fig. 3a–d). At 120 °C, α-Bi_2O_3 is a sole product (Fig. 3e).

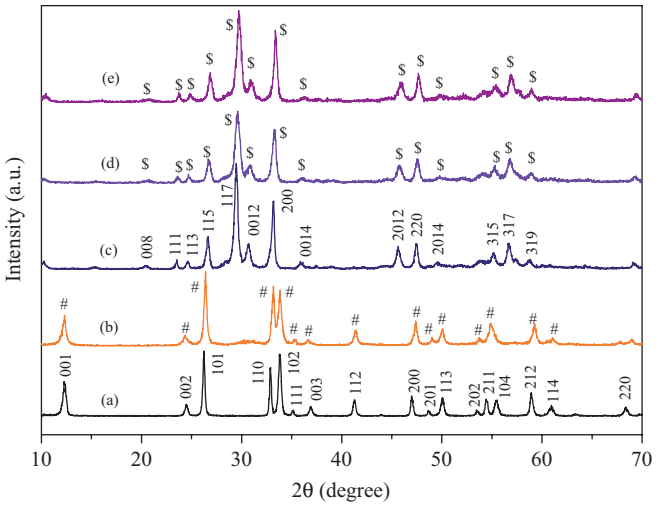

Fig. 1. XRPD patterns of the samples obtained at 120 °C in various mole ratios ($BiCl_3$/NaOH): (a) no NaOH, (b) 1:2, (c) 1:4, (d) 1:6, and (e) 1:8; #, tetragonal BiOCl and $, tetragonal $Bi_{12}O_{17}Cl_2$.

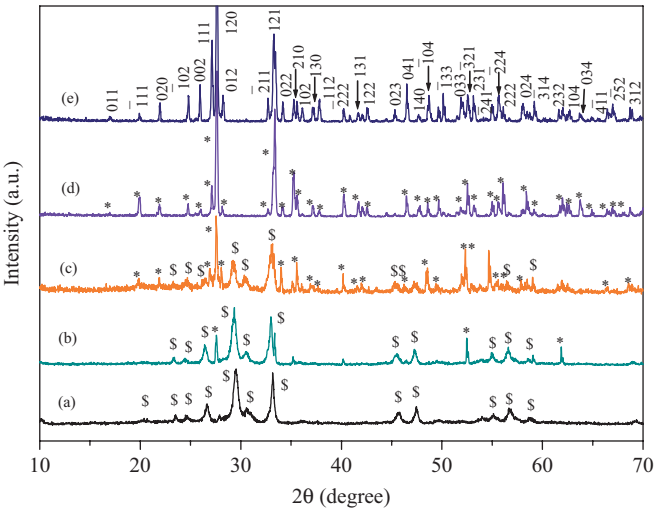

Fig. 2. XRPD patterns of the samples obtained at 120 °C as a function of mole ratio ($BiCl_3$/NaOH): (a) 1:10, (b) 1:12, (c) 1:14, (d) 1:16, and (e) 1:18; $, tetragonal $Bi_{12}O_{17}Cl_2$ and *, monoclinic α-Bi_2O_3 (JCPDS 41-1449).

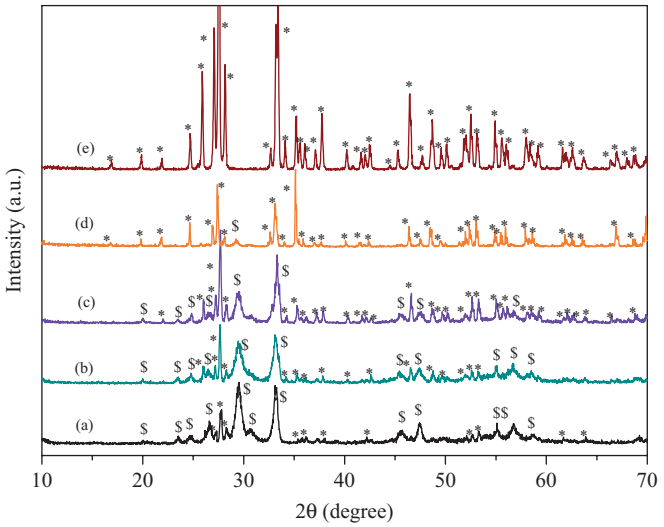

Fig. 3. XRPD patterns of the samples obtained at various temperatures in a fixed mole ratio ($BiCl_3$/NaOH) of 1:18: (a) 40, (b) 60, (c) 80, (d) 100, and (e) 120 °C; $, tetragonal $Bi_{12}O_{17}Cl_2$ and *, monoclinic α-Bi_2O_3.

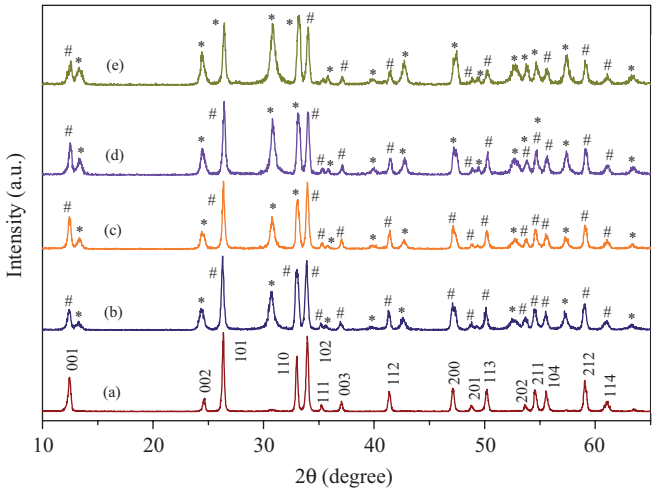

Fig. 4. XRPD patterns of the samples obtained at 120 °C in various mole ratios ($BiCl_3$/urea): (a) 1:2, (b) 1:4, (c) 1:6, (d) 1:8, and (e) 1:10; #, tetragonal BiOCl and *, tetragonal $(BiO)_2CO_3$.

In general, the bismuth metal coexists with other elements in nature to form oxide (Bi_2O_3), carbonate ($(BiO)_2CO_3$), and sulfide (Bi_2S_3), because Bi(III) ion has a high affinity for oxygen and sulfur in aqueous solution [11]. Nonetheless, there has been little exploration on the preparation of $(BiO)_2CO_3$ in the laboratory, except for the aforementioned $(BiO)_2CO_3$ nanotubes synthesized at 200 °C in ethylene glycol [10]. On this basis, we decided to systematically investigate the controlled preparation of $(BiO)_2CO_3$ by using urea as a precipitating agent as well as a base. Fig. 4 shows the XRPD patterns of the samples prepared at 120 °C in various mole ratios ($BiCl_3$/urea). In the mole ratio of 1:2, pure tetragonal BiOCl (JCPDS 06-0249) is formed (Fig. 4a). On the other hand, some reflection peaks assignable to tetragonal $(BiO)_2CO_3$ occur on the XRPD spectrum of the sample prepared in the mole ratio of 1:4 (Fig. 4b). As the mole ratio increases from 1:6 to 1:20, the $(BiO)_2CO_3$ content in the product increases (Figs. 4c–e and 5a–c). If the mole ratio exceeds 1:30, only the reflection peaks corresponding to tetragonal $(BiO)_2CO_3$ occur in the XRPD pattern (Fig. 5d and e). These results strongly indicate the higher mole ratio is favored toward the formation of tetragonal $(BiO)_2CO_3$.

We also examined the reactions by using ammonia in place of urea. Fig. 6 shows the XRPD patterns of the samples obtained at 120 °C as a function of mole ratio ($BiCl_3$/ammonia). In the mole ratio of 1:5, pure tetragonal BiOCl is formed (Fig. 6a). In the mole ratio range of 1:10–1:20, a mixture of tetragonal BiOCl (major) and tetragonal $Bi_{12}O_{17}Cl_2$ (minor) is obtained (Fig. 6b–d).

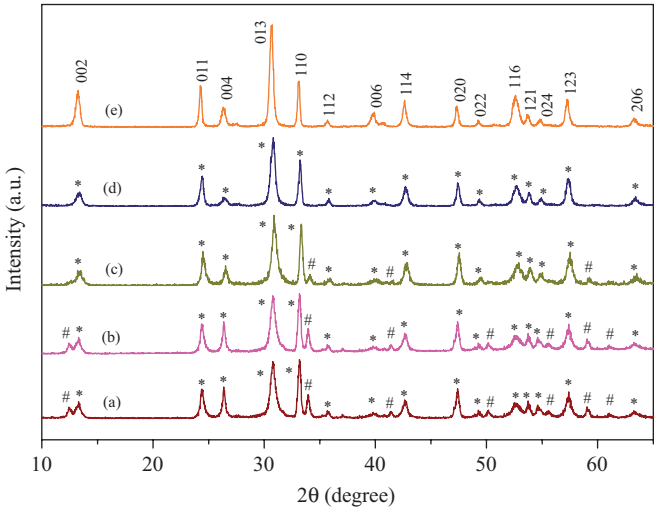

Fig. 5. XRPD patterns of the samples obtained at 120 °C as a function of mole ratio ($BiCl_3$/urea): (a) 1:12, (b) 1:16, (c) 1:20, (d) 1:30, and (e) 1:40; #, tetragonal BiOCl and *, tetragonal $(BiO)_2CO_3$.

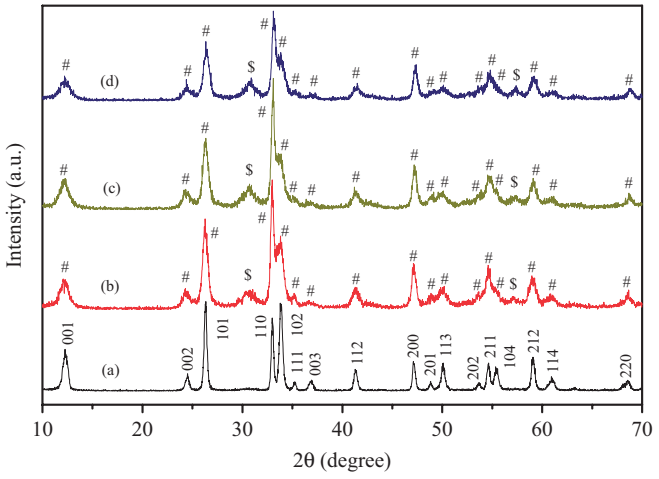

Fig. 6. XRPD patterns of the samples obtained at 120 °C for 12 h in various mole ratios ($BiCl_3$/ammonia): (a) 1:5, (b) 1:10, (c) 1:15, and (d) 1:20; #, tetragonal BiOCl and $, tetragonal $Bi_{12}O_{17}Cl_2$.

Consequently, we could not prepare the pure Bi_2O_3 sample in the presence of ammonia, quite different from those cases employing NaOH. The reason may be due to the fact that ammonia is a relatively weak base ($pK_a = 9.25$) and therefore cannot convert BiOCl into α-Bi_2O_3 under the present conditions.

TEM and HRTEM analyses were performed to investigate the morphologies, sizes, and intrinsic structures of the samples (BiOCl, $Bi_{12}O_{17}Cl_2$, and α-Bi_2O_3). Fig. 7a shows the representative TEM image of the BiOCl sample prepared in the absence of NaOH, illustrating its irregular sheet-like morphology with the nanometer-size thickness. The HRTEM image (Fig. 7b), randomly taken from the BiOCl nanosheets, illustrates their intrinsic structures. The spacing of 0.27 nm between adjacent lattice planes corresponds to that of the (1 1 0) planes of BiOCl crystals.

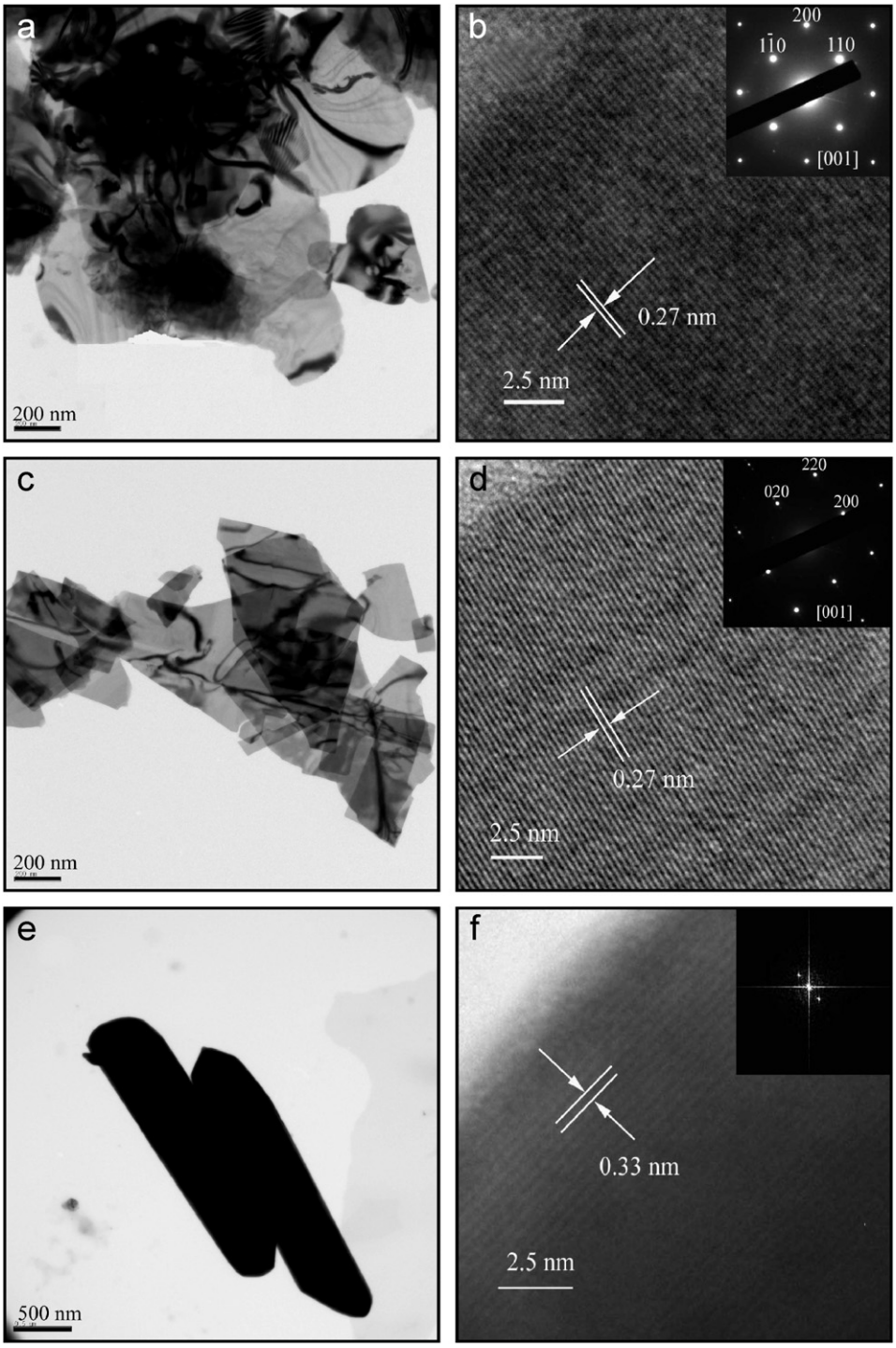

Fig. 7. TEM and HRTEM images of the samples obtained at 120 °C in various mole ratios ($BiCl_3$/NaOH): (a, b) BiOCl (no NaOH), (c, d) $Bi_{12}O_{17}Cl_2$ (1:8), and (e, f) α-Bi_2O_3 (1:18).

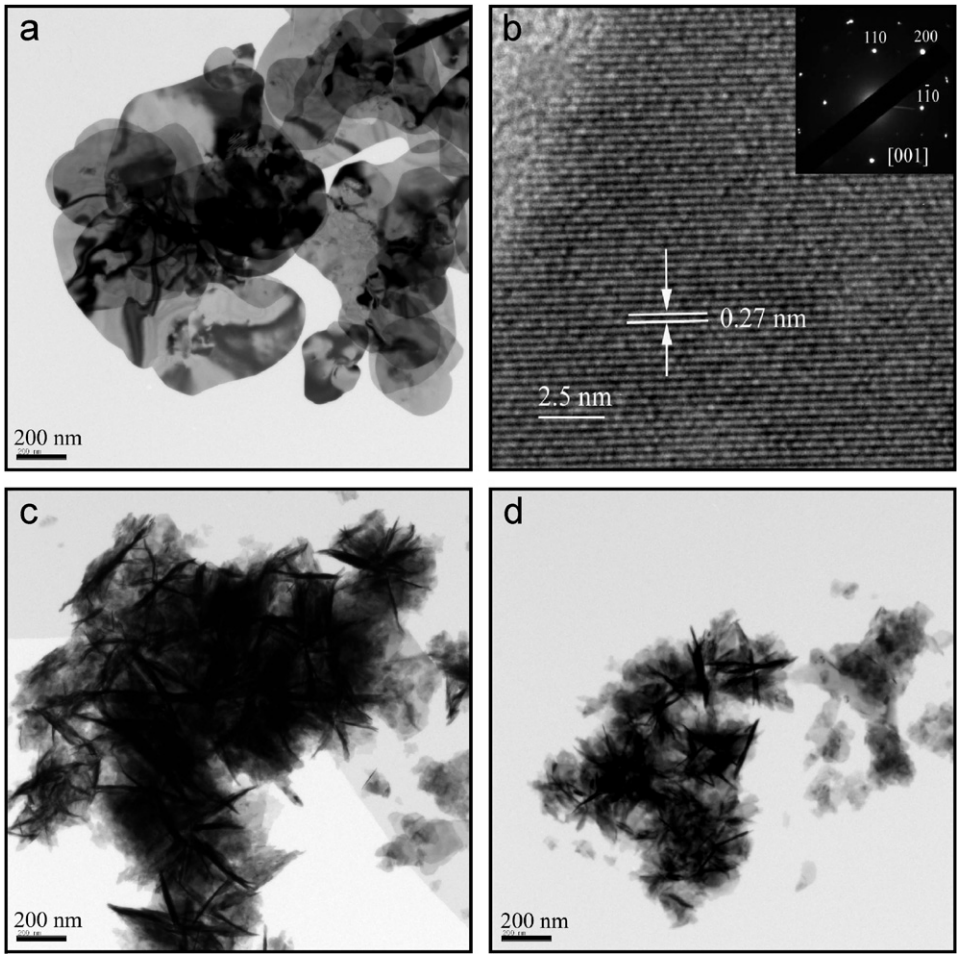

Fig. 8. TEM and HRTEM images of the samples obtained at 120 °C in various mole ratios: (a, b) $(BiO)_2CO_3$ ($BiCl_3$/urea, 1:30) and (c, d) BiOCl ($BiCl_3$/ammonia, 1:15).

The corresponding SAED pattern (the inset of Fig. 7b) demonstrates the single crystal nature of these BiOCl nanosheets. The typical TEM image of $Bi_{12}O_{17}Cl_2$ sample prepared in the mole ratio ($BiCl_3$/NaOH) of 1:8 is presented in Fig. 7c, which reveals that it is composed of many nanosheets. Fig. 7d displays the corresponding HRTEM image with the lattice spacing of 0.27 nm, consistent with that of the (2 0 0) planes of $Bi_{12}O_{17}Cl_2$ crystals. The inset of Fig. 7d further confirms the crystallinity of the as-prepared $Bi_{12}O_{17}Cl_2$ nanosheets with the crystal zone axis of [0 0 1]. Bismuth oxychlorides are known to have a 2-D layer structure, which consists of a chloride ion layer and a metal oxygen layer [5]. Consistent with this fact, the as-prepared BiOCl and $Bi_{12}O_{17}Cl_2$ nanosheets also exhibit preferential growth in the 2-D planar form perpendicular to the *c*-axis. The TEM image of α-Bi_2O_3 sample prepared in the mole ratio ($BiCl_3$/NaOH) of 1:18 is given in Fig. 7e, which illustrates sub-micrometer rods. The HRTEM image in Fig. 7f taken from the edge of the α-Bi_2O_3 rod shows the lattice spacing of 0.33 nm, corresponding to that of the (1 1 1) planes of the α-Bi_2O_3 crystal.

The TEM image of the $(BiO)_2CO_3$ sample prepared in the mole ratio ($BiCl_3$/urea) of 1:30 is presented in Fig. 8a, which also demonstrates its sheet-like morphology. The HRTEM image (Fig. 8b) shows the fringe spacing of 0.27 nm, corresponding to the spacing of the (1 1 0) planes of $(BiO)_2CO_3$. The SAED pattern (inset of Fig. 8b) confirms the crystalline character of the $(BiO)_2CO_3$ nanosheets, also perpendicular to the *c*-axis. The TEM images of the BiOCl sample obtained in the mole ratio ($BiCl_3$/ammonia) of 1:15 are shown in Fig. 8c and d, illustrating lots of irregular nanosheets. From the TEM and HRTEM analyses, we can draw a conclusion that the morphology of BiOCl prepared in the presence of ammonia are somewhat different from those prepared in the absence of NaOH (Fig. 7a and b). All phases and morphologies of the bismuth-based compounds and reaction conditions in this study are summarized in Table 1.

We examined the optical properties of the as-prepared rod-like α-Bi_2O_3 sample. The band gap (E_g) of α-Bi_2O_3 bulk crystal is known to be 2.85 eV at 300 K [25]. Because the present α-Bi_2O_3 sample has the dimensions of sub-micrometers, we do not expect that its E_g value is significantly different from that of the bulk counterpart. Fig. 9 shows the room-temperature PL spectrum of the α-Bi_2O_3

Table 1
Summary of reaction conditions and morphologies for bismuth oxides or oxychlorides prepared at 120 °C in various mole ratios

Sample	Reactants	Initial mole ratio	Phase	Morphology
1	$BiCl_3$	No NaOH	BiOCl	Nanosheets
2	$BiCl_3$ + NaOH	1:2	BiOCl	Nanosheets
3	$BiCl_3$ + NaOH	1:4–1:10	$Bi_{12}O_{17}Cl_2$	Nanosheets
4	$BiCl_3$ + NaOH	1:12–1:14	$Bi_{12}O_{17}Cl_2$ + α-Bi_2O_3	Mixture
5	$BiCl_3$ + NaOH	1:16–1:18	α-Bi_2O_3	Sub-micrometer rods
6	$BiCl_3$ + urea	1:2	BiOCl	Nanosheets
7	$BiCl_3$ + urea	1:4–1:20	BiOCl + $(BiO)_2CO_3$	Nanosheets
8	$BiCl_3$ + urea	1:30–1:40	$(BiO)_2CO_3$	Nanosheets
9	$BiCl_3$ + ammonia	1:5	BiOCl	Nanosheets
10	$BiCl_3$ + ammonia	1:10–1:20	BiOCl + $Bi_{12}O_{17}Cl_2$	Nanosheets

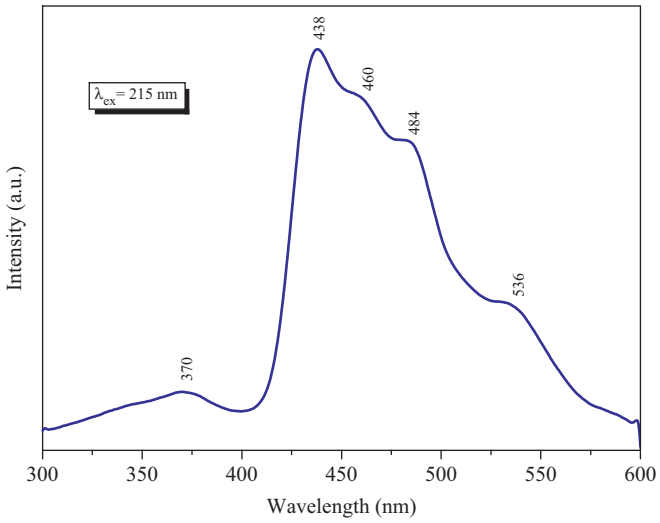

Fig. 9. Room-temperature PL spectrum at $\lambda_{ex} = 215$ nm of the Bi_2O_3 sample prepared at 120 °C in the mole ratio ($BiCl_3$/NaOH) of 1:18.

sample with an excitation wavelength of 215 nm. The curve displays several emission bands: one sharp and strong band at 438 nm (2.83 eV) as well as four weak bands at 370 (3.35 eV), 460 (2.70 eV), 484 (2.56) and 536 nm (2.31 eV). Despite the band gap of the bulk α-Bi_2O_3 (2.85 eV), the present rod-like α-Bi_2O_3 sample does not exhibit the obvious blue or red shift, maybe due to its relatively large size.

In summary, we developed a facile solution-phase synthetic route to BiOCl, $Bi_{12}O_{17}Cl_2$, α-Bi_2O_3, and $(BiO)_2CO_3$ nanoscale crystals. Growth parameters, including reaction temperature, initial mole ratios, and the base species (NaOH, urea, or ammonia), were systematically investigated. BiOCl nanosheets were prepared in the absence of any basic source. $Bi_{12}O_{17}Cl_2$ nanosheets could be synthesized in the mole ratio ($BiCl_3$/NaOH) range of 1:4–1:10. Whereas, rod-like α-Bi_2O_3 was fabricated in the mole ratio ($BiCl_3$/NaOH) of 1:18, $(BiO)_2CO_3$ nanosheets could be prepared in the mole ratio ($BiCl_3$/urea) of 1:30. A mixture of BiOCl and $Bi_{12}O_{17}Cl_2$ was formed in the mole ratio ($BiCl_3$/ammonia) of 1:10–1:20. As expected, the reaction temperature was critical in determining the phases of the final products. The sub-micrometer α-Bi_2O_3 sample exhibited strong emission at room temperature.

Acknowledgment

This work was supported by the Korea Research Foundation Grant funded by the Korean Government (MOEHRD) (KRF-2005-005-J11902).

References

[1] Y.N. Xia, P.D. Yang, Y.G. Sun, Y.Y. Wu, B. Mayers, B. Gates, Y.D. Yin, F. Kim, Y.Q. Yan, Adv. Mater. 125 (2003) 353.
[2] K.H. Park, K. Jang, S.U. Son, Angew. Chem. Int. Ed. 45 (2006) 4608.
[3] C. Zhang, Y.F. Zhu, Chem. Mater. 17 (2005) 3537.
[4] B.Z. Nurgaliev, M.L. Barsukova, V.A. Kuznetsov, B.A. Popovkin, Russ. J. Inorg. Chem. 30 (1985) 948.
[5] N. Kijima, K. Matano, M. Saito, T. Oikawa, T. Konishi, H. Yasuda, T. Sato, Y. Yoshimura, Appl. Catal. A 206 (2001) 237.
[6] D.H. Bao, T.W. Chiu, N. Wakiya, K. Shinozaki, N. Mizutani, J. Appl. Phys. 93 (2003) 497.
[7] B.L. Yu, C.S. Zhu, F.X. Gan, J. Appl. Phys. 82 (1997) 4352.
[8] L.S. Zhang, W.Z. Wang, J.Q. Yang, Z.G. Chen, W.Q. Zhang, L. Zhou, S.W. Liu, Appl. Catal. 308 (2006) 105.
[9] P. Shuk, H.D. Wiemhöfer, U. Guth, W. Göpel, M. Greenblatt, Solid State Ion. 89 (1996) 179.
[10] R. Chen, M.H. So, J. Yang, F. Deng, C.M. Che, H.Z. Sun, Chem. Commun. (2006) 2265.
[11] P.J. Sadler, H.Y. Li, H.Z. Sun, Coord. Chem. Rev. 185–186 (1999) 689.
[12] J. Geng, W.H. Hou, Y.N. Lv, J.J. Zhu, H.Y. Chen, Inorg. Chem. 44 (2005) 8503.
[13] L.Y. Zhu, Y. Xie, X.W. Zheng, X. Yin, X.B. Tian, Inorg. Chem. 41 (2002) 4560.
[14] J. Henle, P. Simon, A. Frenzel, S. Scholz, S. Kaskel, Chem. Mater. 19 (2007) 366.
[15] H. Kodama, S. Horiuchi, A. Watanabe, J. Solid State Chem. 75 (1988) 279.
[16] H. Deng, J.W. Wang, Q. Peng, X. Wang, Y.D. Li, Chem. Eur. J. 11 (2005) 6519.
[17] J.W. Wang, Y.D. Li, Chem. Commun. (2003) 2320.
[18] T. Takeyama, Y. Kajikawa, N. Takahashi, T. Nakamura, S. Itoh, Chem. Vap. Depos. 12 (2006) 203.
[19] H.W. Kim, J.H. Myung, S.H. Shim, Solid State Commun. 137 (2006) 196.

[20] Y.F. Qiu, D.F. Liu, J.H. Yang, S.H. Yang, Adv. Mater. 18 (2006) 2604.
[21] B.J. Yang, M.S. Mo, H.M. Hu, C. Li, X.G. Yang, Q.W. Li, Y.T. Qian, Eur. J. Inorg. Chem. (2004) 1785.
[22] L. Li, Y.W. Yang, G.H. Li, L.D. Zhang, Small 2 (2005) 548.
[23] M.M. Patil, V.V. Deshpande, S.R. Dhage, V. Ravi, Mater. Lett. 59 (2005) 2523.
[24] H.O. Jungk, C. Feldmann, J. Mater. Sci. 36 (2001) 297.
[25] L. Leontie, M. Caraman, M. Alexe, C. Harnagea, Surf. Sci. 507–510 (2002) 480.